ELSEVIER

Materials Chemistry and Physics 77 (2002) 938–944

MATERIALS CHEMISTRY AND PHYSICS

www.elsevier.com/locate/matchemphys

Spray pyrolysis deposition and characterization of titanium oxide thin films

L. Castañeda [a], J.C. Alonso [a], A. Ortiz [a,*], E. Andrade [b], J.M. Saniger [c], J.G. Bañuelos [c]

[a] *Instituto de Investigaciones en Materiales, U.N.A.M. A.P. 70-360, Coyoacán 04510, D.F., Mexico*
[b] *Intituto de Física, U.N.A.M. A.P. 20-364, Coyoacán 04510, D.F., Mexico*
[c] *Centro de Instrumentos, U.N.A.M. A.P. 70-186, Coyoacán 04510, D.F., Mexico*

Received 11 December 2001; received in revised form 18 April 2002; accepted 27 April 2002

Abstract

Titanium oxide films were deposited by the ultrasonic spray pyrolysis process using titanium oxide acetylacetonate (TAAc) as source material dissolved in pure methanol. As-deposited films show the anatase crystalline structure, while annealed samples at 850 °C have the rutile phase. Rutherford backscattering measurements indicate that the deposited films are formed by stoichiometric TiO_2 material. Root-mean-square (rms) roughness depends on the substrate temperature and on the annealing process. Refractive index has values of the order of 2.36 for as-deposited films and 2.698 for annealed films. This change is associated with the anatase to rutile phase change. IR analyses show well-defined absorption peaks located at 433 and 638 cm^{-1} for anatase phase and peaks located at 419, 466, 499 and 678 cm^{-1} for rutile phase. In general, the titanium oxide films show high optical transmission. The energy band gap calculated for the anatase phase is of the order of 3.4 eV. The current density–electric field characteristics of MOS structures show current injection across the titanium oxide film even for low applied electric fields. However, electric breakdown was not observed for applied fields up to 5 MV cm^{-1}.

Keywords: Thin films; Titanium oxide; Pyrosol

1. Introduction

Titanium oxide has three different crystalline phases: brookite, anatase and rutile. Among them, the brookite phase has an orthorhombic crystalline structure. However, this is an unstable phase and it is of low interest. Both anatase and rutile phases have a tetragonal crystalline structure. The anatase and rutile are stable phases with mass densities of 3.84 and 4.26 g cm^{-3}, respectively [1]. In general, the rutile phase is formed at high temperatures, while the anatase phase is formed at low temperatures.

Due to their electrical properties: high dielectric constant and high resistivity, their optical properties: high refractive index and high optical transparency over a wide spectral range, and their mechanical properties: relatively high hardness, titanium oxide thin films have several possible applications like electric insulator and protective layers in electronic devices, antireflective and protective layers for optical coatings, wear resistant coatings, etc. [2–5].

On the other hand, titanium oxide is a polar material used as a substrate in catalytical and electrochemical processes. These features make titanium oxide potentially suitable as gas sensing material. The electrical conductivity of titanium oxide and platinum–titanium oxide changes with the composition of the gas atmosphere surrounding them. These gas sensors have been used to detect NH_3, H_2, O_2 and hydrocarbons in air and vacuum [6,7].

There are several oxide compounds such as $SrTiO_3$, $PbTiO_3$ and Sr(Zr, Ti)O_3, which have large figure of merit (defined by the product of $\varepsilon_0\varepsilon_r E_b$, where ε_r is the relative dielectric constant, ε_0 the permittivity of free space and E_b the breakdown electric field) for applications as insulating layers in alternating current electroluminescent devices [8]. Titanium oxide and the above mentioned oxide compounds have large enough band gap suitable for that application.

Titanium oxide films have been prepared by several techniques, using different titanium source materials, such as anodization [9], activated reactive evaporation [10], reactive dc magnetron sputtering [11], pulsed laser reactive evaporation [12], ion beam sputtering [13], plasma enhanced chemical vapor deposition [14], and spray pyrolysis [15]. Probably, the spray pyrolysis technique is the cheapest and easiest process to prepare thin films. This technique has been used to deposit insulating and active device layers [16,17] and it is suitable to prepare metallic oxide films over

* Corresponding author. Tel.: +52-5622-4599; fax: +52-5616-1201.
E-mail address: aortiz@servidor.unam.mx (A. Ortiz).

0254-0584/02/$ – see front matter
PII: S0254-0584(02)00193-1

large area. It does not need vacuum systems because the films are deposited at air atmosphere. Metallic oxide films prepared by spray pyrolysis for different applications have shown homogeneous properties on relatively large areas. Thin films of titanium oxide containing Li and Nb have been prepared by spray pyrolysis using an aqueous solution of titanium peroxo–hydroxo-complex as titanium source material. However, the obtained deposition rate, in that case, is too low for device manufacture applications [15].

Our main interest is to prepare titanium oxide thin films with structural and electrical characteristics suitable for gas sensing applications and, on the other hand, as a first step to produce oxide compounds with large figure of merit for electroluminescent device preparation. In this work, we report the structural, optical and electrical properties of titanium oxide films prepared by ultrasonic spray pyrolysis technique using titanium oxide acetylacetonate (TAAc) as titanium source material. With this titanium source material it is possible to obtain deposition rates high enough for device manufacture applications.

2. Experimental

Titanium oxide thin films were prepared by the ultrasonic spray pyrolysis technique [16]. The start solution was 0.05 M TAAc, from Aldrich, in pure methyl alcohol. The substrate temperature (T_s) was varied from 200 to 550 °C in 25 °C steps. Filtered air was used as carrier and director gas, the air flow rates were 3.5 and 0.5 l min^{-1}, respectively. The deposition time was 7.5 min in all cases. In order to promote the crystallization in the rutile phase, some of the samples were annealed at 650, 750, 850 and 950 °C in air atmosphere for 1 h. For X-ray diffraction, surface morphology and optical measurements the used substrates were clear fused quartz slices ultrasonically cleaned with trichloroethylene, acetone and methyl alcohol. For profilometry measurements Pyrex glass slices, cleaned in a similar way as the above mentioned case, were used as substrates. A small part of these substrates was covered with a cover glass slice to get an step during deposition. For ellipsometry, infrared (IR) spectroscopy, and ion beam elemental composition measurements (1 0 0) n-type silicon single crystalline wafers with 200 Ω cm were used as substrates. To remove the native oxide from the c-Si wafers, they were chemically etched with P solution (15 parts of HF, 10 parts of HNO_3 and 300 parts of H_2O). Meanwhile for current–voltage measurements of as-deposited films, they were incorporated in a MOS structure using (1 0 0) n-type silicon single crystal wafers with 0.2 Ω cm as substrates. The top electrodes onto the titanium oxide films were aluminum dots with 1.38 mm diameter deposited by thermal evaporation through a metallic mask.

The crystallinity of as-deposited and annealed samples was analyzed by means of X-ray diffraction measurements with a Siemens D500 diffractometer using the Cu Kα1 wavelength (1.54056 Å). The atomic force studies were performed with a Park AutoProbe CP equipment. The deposited samples were imaged in contact mode using a Si Ultralever^{TM} tip with a force of 0.26 N m^{-1} and resonant frequency of 40 kHz, the applied force used for scanning the surface was 8 nN. The images presented here were submitted only to a flatness process. Roughness and other geometric parameters of the surface were measured on the original images before the flatness processing. The elemental composition of deposited titanium oxide films was obtained using the ion beam analysis (IBA) facilities at the University of México, based on a vertical single ended 5.5 MeV Van de Graaff accelerator. A conventional Rutherford backscattering technique with a 2 MeV $^4He^+$ beam with detector set at $\theta = 170°$ was used to analyze the films. A surface barrier detector and standard electronics were used to obtain the particle energy spectra. The thickness of the deposited films onto Pyrex glass was measured with a Sloan Dektac IIA profilometer on the step formed during deposition. The refractive index n and thickness of as-deposited and annealed films were measured with a Gaertner 117A ellipsometer using the 632 nm line from a He–Ne laser. IR transmittance measurements were made with a Fourier transform IR (FTIR) 205 Nicolet spectrophotometer. Similarly, optical transmission measurements in the range from 190 to 1100 nm were made with a double beam Shimadzu UV–Vis 260 spectrophotometer with air in the reference beam. The current–voltage characteristics were measured in an automated system with a programmable Keithley 230 voltage source and a Keithley 580 logarithmic picoammeter controlled by a PC.

3. Results and discussion

From the X-ray measurements it was observed that samples prepared at T_s lower than 300 °C are of amorphous nature. This result is in agreement with anatase phase crystallization temperature of about 300 °C [18]. The as-deposited samples with $T_s \geq 300$ °C and the annealed samples show a polycrystalline microstructure as shown in Fig. 1. The X-ray diffraction spectrum from a sample deposited at substrate temperature of 450 °C (Fig. 1a) corresponds to anatase tetragonal crystalline structure (ASTM card 21-1272), which is normally obtained at low temperatures as reported [19]. X-ray spectra obtained for all the as-deposited samples correspond to the anatase phase. In all these cases the peak with highest intensity is associated with reflection from the (1 0 1) family planes. The main difference in these spectra is the magnitude of the diffraction peak, which increases as the substrate temperature increases. This fact can be explained by considering that at higher substrate temperature the adsorbed radicals have higher surface kinetic energy, which permits them a better accommodation to the deposited material with larger grain size and a preferential orientation of the crystalline structure. It should be remarked that X-ray diffraction spectra of samples annealed

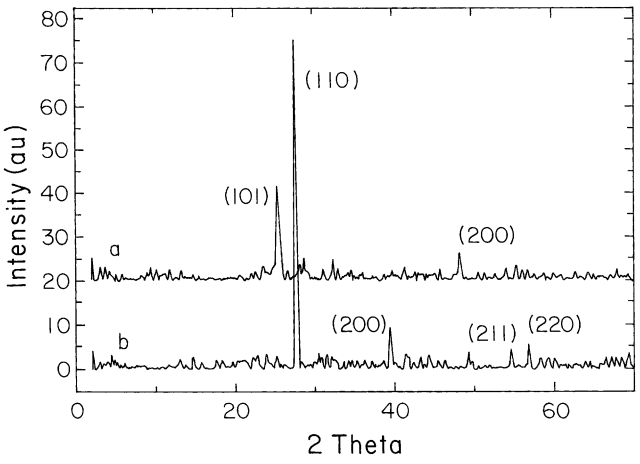

Fig. 1. X-ray diffraction spectra for a titanium oxide films: (a) as-deposited at 450 °C and (b) annealed at 850 °C.

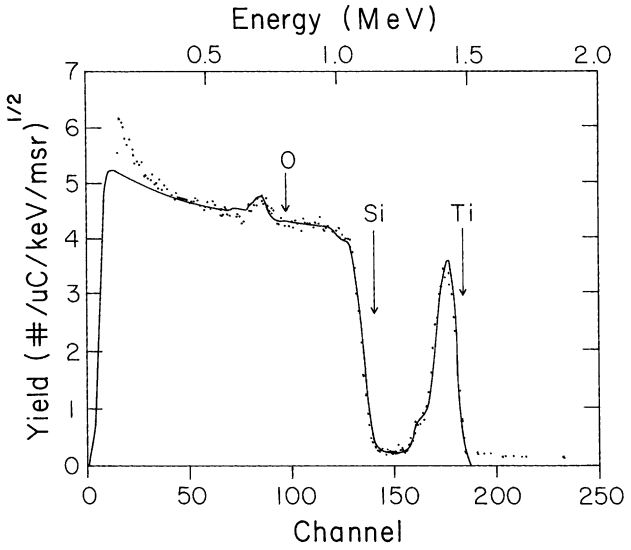

Fig. 2. A 2 MeV $^4He^+$ backscattered spectrum (dots) from a titanium oxide film over silicon substrate. Scattering geometry is set up for normal incidence and the laboratory angle 170°. The solid line is the RUMP simulated spectrum.

at 650 and 750 °C, even show the same diffraction peaks associated with the anatase phase, the peaks present higher intensities than those observed for the as-deposited samples, which could be associated with a grain growth effect. However, no peaks related with rutile phase were observed as reported for samples annealed at these temperatures [20]. Fig. 1b shows that the X-ray diffraction spectrum for a sample annealed at 850 °C corresponding to rutile tetragonal crystalline structure (ASTM card 21-1276), which is the high temperature stable phase of the titanium oxide. A similar spectrum is obtained for the sample annealed at 950 °C. The X-ray spectra for samples annealed at high temperature show only one peak associated with reflection from the close packed (1 1 0) family plane of the rutile phase and the reflection from (1 0 1) planes, which has the highest intensity in spectra of as-deposited films with anatase crystalline structure is missed. This fact can be explained by taking into account the crystalline phase transformation due to annealing process resulting in a preferential orientation of the rutile crystalline structure textured along (1 1 0) planes. The observed change of the crystalline structure due to annealing at temperatures of the order of 850 °C is in agreement with several reports [21,22]. The thickness of the deposited films, measured by ellipsometry, varies in the range from 200 to 230 nm. However, it does not show the trend normally observed for films deposited by the spray pyrolysis technique, where the thickness of the deposited films decreases as the substrate temperature increases. This fact can be explained by taking into account that the titanium source material being a metallorganic titanium oxide contains TiO radicals. The Ti–O radicals are produced due to decomposition of the titanium material source during the transit of the solution drops towards the surface of the substrate. These Ti–O radicals are adsorbed on the surface of the substrate and they are not evaporated to the vapor phase because the titanium monoxide boiling temperature is high (≅3000 °C) [1]. The oxidation of these radicals to form TiO_2 must be almost completed even at low substrate temperature.

Fig. 2 shows a typical backscattered $^4He^+$ spectrum of 2 MeV ions incident at 0° angle respect to the normal of the titanium oxide film deposited on a single crystalline silicon wafer at 550 °C. In this spectrum it can be observed that signals associated with titanium, oxygen, and silicon, without any signal related with carbon from the material source. Similar spectra were obtained for all the deposited samples. A quantitative analysis of the RBS spectra was made using the well-known "RUMP" software [23]. The analysis consists of a simulation of the spectrum (solid line) and its comparison with experimental ones (dots). In the present case three layers were needed to simulate the experimental spectrum. The front layer thickness is 5×10^{17} atoms cm^{-2} with a stoichiometric composition of TiO_2. The second layer is a transition layer with 3×10^{17} atoms cm^{-2} and composition of $Ti_{0.8}O_{1.0}Si_{1.5}$. The third layer is the silicon substrate. The RUMP errors for titanium and oxygen determination are about 8%.

Fig. 3 shows the three-dimensional AFM image of the surface of TiO_2 film prepared at $T_s = 500$ °C, on a clear fused quartz substrate, having anatase crystalline structure. Fig. 4 shows the three-dimensional AFM image of the surface of a titanium oxide film annealed at 850 °C having rutile structure. It should be noted that these images could indicate that the surface of the deposited films are textured in both cases. In Fig. 4, it appears that it is possible to observe grains with size of about 4 μm. The root-mean-square (rms) roughness of the samples obtained with a substrate temperature between 400 and 550 °C decreases as a function of the increase of T_s (rms roughness of 11.4 nm for $T_s = 400$ °C and 4.2 nm for $T_s = 500$ °C). This fact can be explained by considering that at a given substrate temperature the deposition of films is carried out by a real chemical vapor deposition

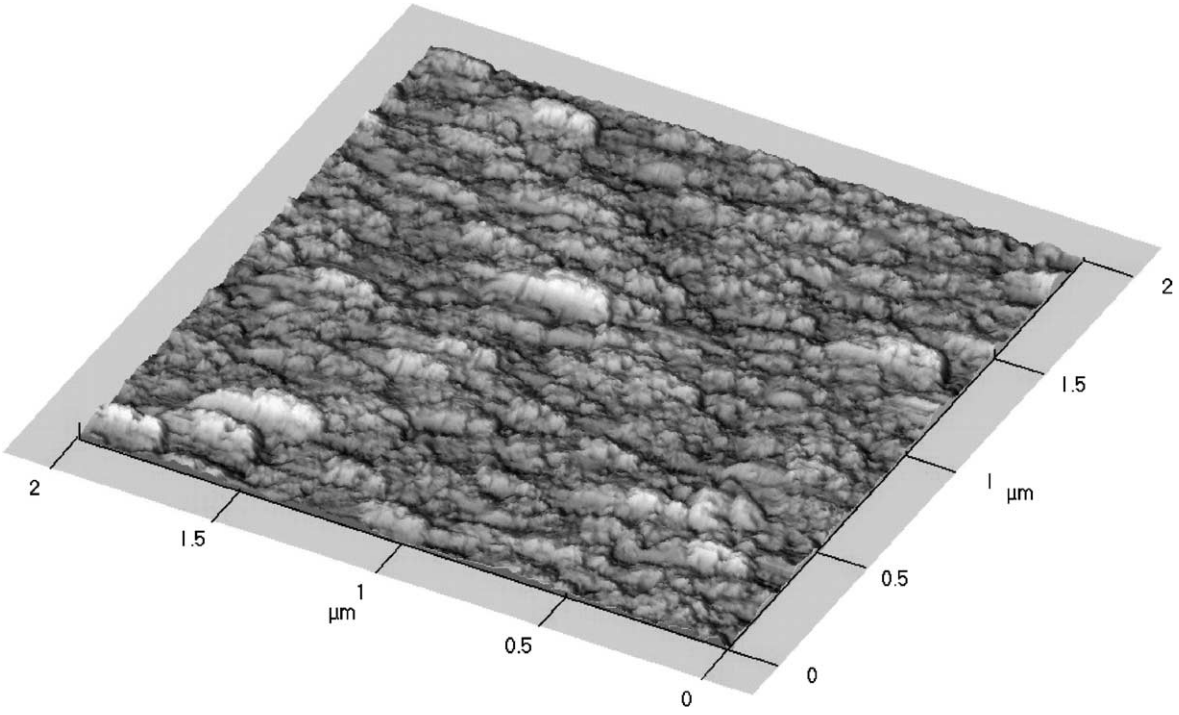

Fig. 3. A three-dimensional AFM image of as-deposited titanium oxide film grown at 500 °C on quartz substrate.

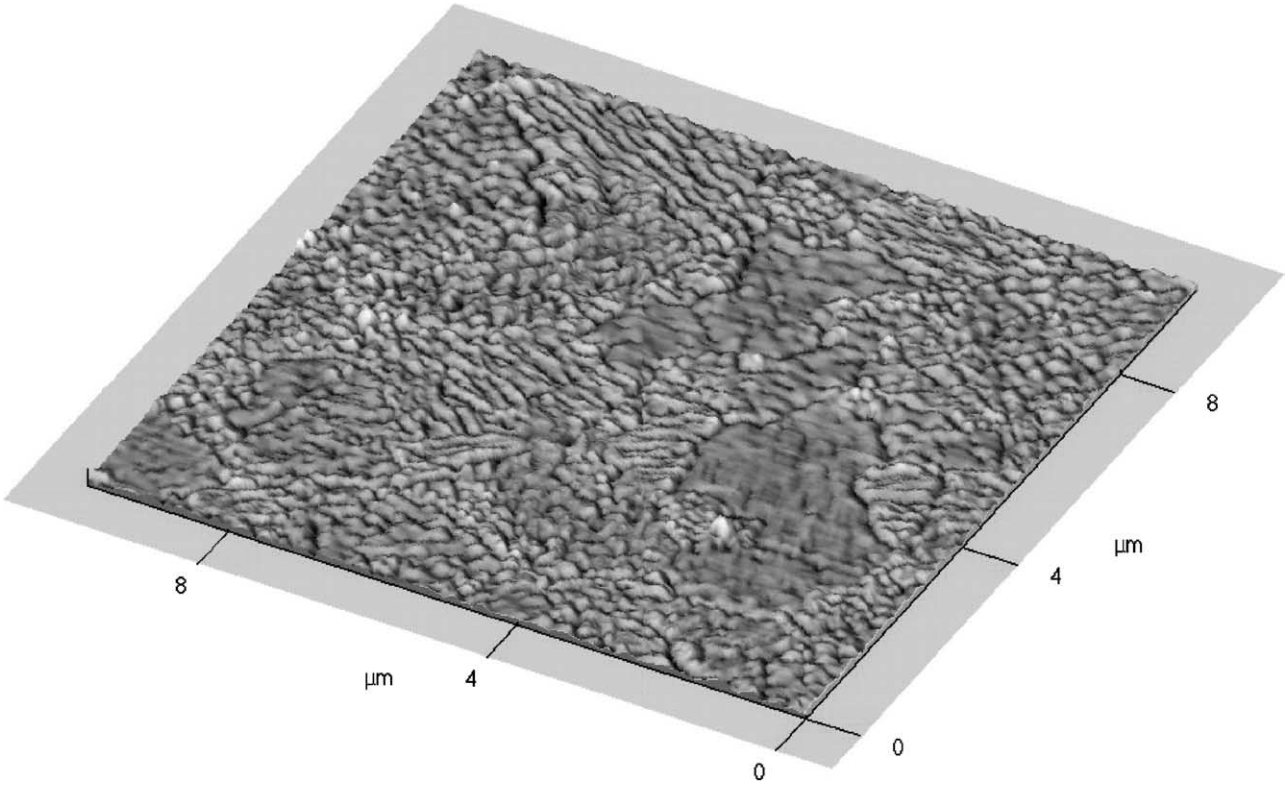

Fig. 4. A three-dimensional AFM image of titanium oxide film annealed at 850 °C.

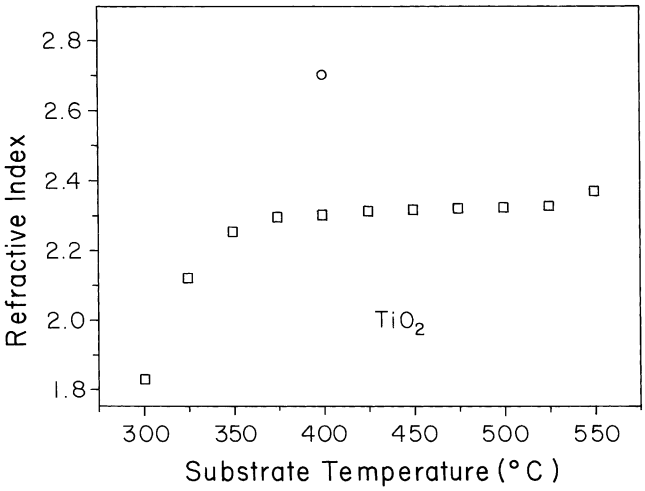

Fig. 5. Refractive index as a function of substrate temperature for as-deposited titanium oxide films prepared by spray pyrolysis (open square). It is also shown the refractive index for a film annealed at 850 °C (open circle).

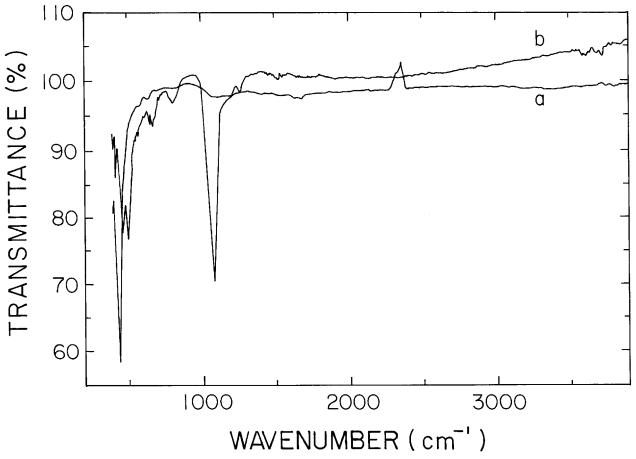

Fig. 6. IR transmittance spectra of titanium oxide films: (a) as-deposited at $T_s = 550\,^{\circ}C$ and (b) film annealed at 950 °C.

process through heterogeneous chemical reactions with the film growing by means of an atomistic process. Then, at higher T_s the adsorbed radicals have higher surface mobility resulting in a better accommodation and in a smoother surface of the deposited film. On the other hand, when a sample deposited at $T_s = 500\,^{\circ}C$ was additionally annealed at 850 °C in order to induce the anatase–rutile phase transformation (Fig. 4), an increase of the rms roughness values from 4.22 to 7.74 nm was observed. This result could be associated with the phase transformation, which implies a significant increase of the density [1] and the grain growth effects.

Fig. 5 shows that the refractive index for deposited films with T_s from 300 to 550 °C takes values in the range from 1.825 to 2.381. The refractive index reaches an almost constant value of 2.36 for samples prepared at substrate temperature ranging from 375 to 525 °C. The increase of the refractive index values as a function of the substrate temperature is associated with a densification effect of the deposited films as T_s increases (due to higher surface mobility of the adsorbed species at higher T_s). This observed trend is in agreement with X-ray diffraction results where the magnitude of the diffraction peaks increases as T_s increases due to a grain growth effect. These n values are in agreement with those previously reported for TiO_2 [24]. Occasional higher refractive index values reported in the literature are associated with poorly oxidized titanium oxide films [25]. The amorphous samples, in the present case, have refractive index values of about 2.076, which is of the same order of those measured for crystalline samples prepared at higher substrate temperatures indicating that the amorphous deposited samples are formed by a poorly oxidized material. This fact can be explained by taking into account that the titanium source material has TiO radicals. At low T_s the incorporation of non-oxidized TiO radicals results in higher refractive index values due to a metal-rich deposited material, even though the samples being of amorphous nature are formed by low density material. Similar refractive index values (≅2.36) were obtained for the samples annealed at 650 and 750 °C, which do not change their crystalline structure from anatase phase to rutile one. On the other hand, Fig. 5 also shows the refractive index for the sample annealed at 850 °C (open circle) with a value of 2.698. This value is similar to that reported (≅2.7) for the rutile phase of titanium oxide obtained in annealed samples [25]. Although both anatase and rutile phases have tetragonal crystalline structure, there is a difference in the lattice parameter being the anatase phase less dense than the rutile phase. This fact explains the difference in the refractive index values for these phases.

Fig. 6 shows the IR spectra for an as-deposited sample at substrate temperature of 550 °C (Fig. 6a) and for a sample annealed at 950 °C (Fig. 6b). The transmittance spectrum of the as-deposited sample shows a main absorption band centered at 433 cm^{-1} and several small features located at 638, 804 and 1076 cm^{-1}. The absorption bands located at 804 and 1076 cm^{-1} are related with the bending and stretching vibration modes of the Si–O bond at the interface region [26] which is formed by the diffusion of oxygen into the silicon substrate as observed from the RBS measurements. The absorption bands located at 433 and 638 cm^{-1} can be associated to Ti–O bond vibrations. However, it is worth to mention that they do not match with the positions previously reported at 514 and 696 cm^{-1} for the anatase phase of titanium oxide, which are related to stretching vibration of the Ti–O bond for tetrahedral and octahedral surroundings of the titanium atom, respectively [27,28].

The IR spectrum for the annealed sample shows several well-defined absorption bands located at 419, 466, 499, 678, 809, 1080 and 1268 cm^{-1}. The absorption bands located at 466, 809 and 1080 cm^{-1} are related to the rocking, bending

and stretching vibration modes of the Si–O bond in the interface region. The magnitudes of these bands are higher than those observed in spectrum of Fig. 6a, which is associated with a strong diffusion of oxygen into the silicon substrate developing a wide interface region due to the relatively high annealing temperature. All the other absorption bands can be related to vibrations of the Ti–O bond. However, the absorption bands reported for the rutile phase are located at 423, 615 and 697 cm^{-1} [29]. Given these results for both anatase and rutile phases, more work is necessary to clarify the observed difference in location of the absorption peaks.

On the other hand, it should be remarked that, in both spectra, there are no absorption signals between 2600 and 3800 cm^{-1} related to incorporated OH groups as reported for overstoichiometric titanium oxide [28]. This fact indicates that both the as-deposited and the annealed samples are formed by dense materials without porous.

Fig. 7 shows the optical transmission spectra for two as-deposited films with substrate temperatures of 400 (Fig. 7a) and 550 °C (Fig. 7b) and for a film annealed at 950 °C (Fig. 7c). The transmission spectra for a clear fused quartz substrate, similar to those used to deposition, is also shown (Fig. 7d). From Fig. 7a and b spectra for the as-deposited films it can be observed a small shift of the absorption edge toward larger wavelengths. This result is in agreement with results reported earlier [28,30]. In general, the increase of the substrate temperature promotes grain growth and the absorption edge is shifted towards longer wavelength as observed in the present case. The observed shift towards longer wavelength for the annealed sample (Fig. 7c) can be explained in the same way. In the annealed samples the deposited films change their crystalline structure from anatase to rutile phase, accompanied by a grain growth process. The shift of the absorption edge towards larger wavelengths is associated, in both cases,

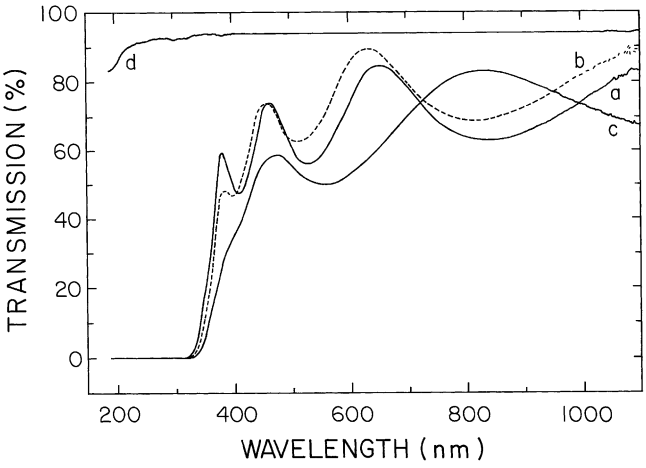

Fig. 7. Optical transmission spectra of titanium oxide films as-deposited at 400 °C (a) and 550 °C (b) and for a film annealed at 950 °C (c). The spectrum of a clear fused quartz (d) similar to that used as substrates is also shown.

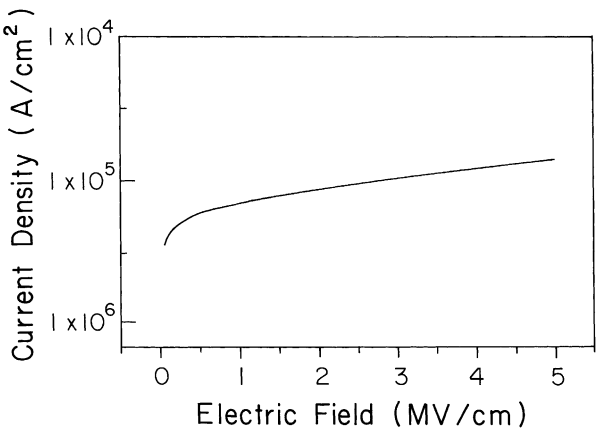

Fig. 8. Current density–electric field characteristic of a MOS structure where an as-deposited titanium oxide film grown at 450 °C is incorporated.

with a grain growth effect due to higher temperature processing of the deposited material. Using the Swanepoel's method [31], the optical band gap was determined for the as-deposited sample considering direct allowed transitions. The determined value of the optical band gap is 3.4 eV, which is of the order of theoretical data and experimental values obtained for crystallized anatase films [32].

Fig. 8 shows the current–voltage characteristics of a MOS structure where an as-deposited titanium oxide film, with $T_s = 450$ °C and thickness of 199.3 nm, was incorporated. From this figure, it can be observed that a step in the current density is established even for low applied electric field, which is associated with a high current injection across the titanium oxide film. However, the current injection increases gradually as the applied electric field increases, without any signal associated with local dielectric breakdown. The electrical conductivity is of the order of 10^{-12} $(\Omega\,cm)^{-1}$. This value appears to be suitable for applications of these films to gas sensor devices [33]. The current density increases up to values of the order of 10^5 A cm^{-2} at electric fields of about 5 MV cm^{-1}. It should be remarked that no destructive breakdown was observed at the high values of current density and electric fields reached.

4. Conclusions

Titanium oxide films were prepared by the ultrasonic spray pyrolysis process using TAAc as source material. The films deposited at substrate temperature lower than 300 °C are of amorphous nature. Films deposited at temperatures in the range from 300 to 550 °C, show the anatase crystalline structure. Meanwhile, samples annealed at 850 °C are formed by material with the rutile phase. In general, the titanium oxide films form with a TiO_2 stoichiometric composition. The surface of the films has an rms roughness depending on the substrate temperature. The refractive index has an almost constant value of the order of 2.36 for

as-deposited films and 2.698 for annealed films, which is associated with the change of phase and a densification effect. The IR spectra show well-defined absorption peaks located at 433 and 638 cm^{-1} for as-deposited samples and peaks located at 419, 466, 499 and 678 cm^{-1} for annealed films. However, these peaks do not correspond to reported values for both phases. It should be remarked that no absorption signals related with OH groups are observed. The optical transmission spectra have a relatively high percentage of transmittance in the wavelength range from 400 to 900 nm. The optical band gap is of the order of 3.4 eV for as-deposited films. The electrical characteristics indicate that the films have electrical conductivity of about $10^{-12}\,(\Omega\,cm)^{-1}$ and that a real current injection across the film is observed even for low applied electric field. Electric breakdown was not observed for electric fields up to 5 $MV\,cm^{-1}$. In summary, titanium oxide films with microstructural and electric characteristics suitable to be applied to gas sensors manufacture have been prepared by spray pyrolysis technique.

Acknowledgements

The authors want to thank M.A. Canseco, L. Baños, L. Huerta, E.P. Zavala and S. Jimenez for technical assistance. This work was partially supported by CONACyT (México) under contract 27635-U and DGAPA-UNAM under project IN101799. The CN accelerator Van de Graaff laboratory operation was partially supported by DGAPA-UNAM under project IN108798.

References

[1] R.C. Weast (Ed.), Hand Book of Chemistry and Physics, 67th Edition, CRC Press, Boca Raton, FL, 1986–1987, p. B-140.
[2] H.K. Hu, M. Yoshimoto, H. Koinuma, B.K. Moon, H. Ishiwara, Appl. Phys. Lett. 68 (1996) 2965.
[3] T. Houzouji, N. Saito, A. Kudo, S. Takata, Chem. Phys. Lett. 254 (1996) 109.
[4] Z. Chen, P. Sana, J. Salami, A. Rohatgi, IEEE Trans. Electron. Dev. 40 (1993) 1161.
[5] H. Kuster, J. Erbert, Thin Solid Films 70 (1980) 43.
[6] R.M. Walton, D.J. Dwyer, J.W. Schwank, J.L. Gland, Appl. Surf. Sci. 125 (1998) 199.
[7] D. Manno, G. Micocci, R. Rella, A. Serra, A. Taurino, A. Tepore, J. Appl. Phys. 82 (1997) 54.
[8] Y.A. Ono, in: G.L. Trigg (Ed.), Electroluminescence, Encyclopedia of Applied Physics, Vol. 5, Wiley-VCR Publishers Inc., Berlin, 1993, p. 295.
[9] J. Pouilleau, D. Devilliers, F. Garrido, S. Duran-Vidal, E. Mahé, Mater. Sci. Eng. B 47 (1997) 235.
[10] T. Fujii, N. Sakata, J. Takata, Y. Miura, Y. Daitoh, M. Takano, J. Mater. Res. 9 (1994) 1468.
[11] P. Alexandrov, J. Koprinarova, D. Todorov, Vacuum 47 (1996) 1333.
[12] L. Shi, H.J. Frankena, H. Mulder, Vacuum 40 (1990) 399.
[13] F. Zhang, X. Lin, S. Jin, H. Bender, N.Z. Lou, Z.H. Wilson, Nucl. Instrum. Meth. Phys. Res. B 142 (1998) 61.
[14] C. Martinet, V. Paillord, A. Gagnaire, J. Joshep, J. Non-Cryst. Sol. 216 (1997) 77.
[15] N. Golego, S.A. Studenikin, M. Cocivera, J. Mater. Res. 14 (1999) 698.
[16] A. Ortiz, J.C. Alonso, V. Pankov, A. Huanosta, E. Andrade, Thin Solid Films 368 (2000) 74.
[17] A. Ortiz, J.C. Alonso, V. Pankov, D. Albarran, J. Luminesc. 81 (1999) 45.
[18] W.G. Lee, S.I. Woo, J.C. Kim, S.H. Choi, K.H. Oh, Thin Solid Films 237 (1994) 105.
[19] D. Leinen, J.P. Espinas, A. Fernandez, A.R. Gonzalez-Elipe, J. Vac. Sci. Technol. A 12 (1994) 5.
[20] M.L. Hitchman, J. Zhao, J. Physique IV 9 (1999) Pr8-357.
[21] W.W. Xu, R. Kershaw, K. Dwight, A. Wold, Mater. Res. Bull. 25 (1990) 1385.
[22] K. Yokota, T. Yamada, F. Miyashita, K. Hirai, H. Takano, M. Kumagai, Thin Solid Films 334 (1998) 109.
[23] L.R. Doolite, Nucl. Instrum. Meth. Phys. Res. B 15 (1986) 227.
[24] N. Martin, C. Rousselot, C. Savall, F. Palmino, Thin Solid Films 287 (1996) 154.
[25] D. Wicaksana, A. Kobayashi, A. Kimbara, J. Vac. Sci. Technol. A 10 (1992) 1479.
[26] J.C. Alonso, R. Vazquez, A. Ortiz, V. Pankov, J. Vac. Sci. Technol. A 16 (1998) 3211.
[27] M.L. Calzada, L. del Olmo, J. Non-Cryst. Sol. 121 (1990) 413.
[28] S. Ben-Amor, G. Band, J.P. Besse, M. Jaquet, Mater. Sci. Eng. B 47 (1997) 110.
[29] J.R. Ferraro, Low Frequency Vibrations of Inorganic and Coordination Compounds, Plenum Press, New York, 1971, p. 72.
[30] F. Zhang, Z. Zheng, X. Ding, Y. Mao, Y. Chen, Z. Zhon, S. Yamg, X. Liu, J. Vac. Sci. Technol. A 15 (1997) 1824.
[31] R. Swanepoel, J. Phys. E 16 (1983) 1214.
[32] A. Amtouth, R. Leonnel, Phys. Rev. B 51 (1995) 6842.
[33] R.M. Walton, D.J. Dwyer, J.W. Schwanh, J.L. Gland, Appl. Surf. Sci. 125 (1998) 199.